Cavitating vortex characterization based on acoustic signal detection

Angela Digulescu, Irina Murgan, Ion Candel, A Bunea, G Ciocan, Diana M Bucur, Georgiana Dunca, Cornel Ioana, Gabriel Vasile, Alexandru M Serbanescu

Cavitating vortex characterization based on acoustic signal detection

A. Digulescu[1,2], I. Murgan[1], I. Candel[1], F. Bunea[3], G. Ciocan[4], D.M. Bucur[5], G. Dunca[5], C. Ioana[1], G. Vasile[1] and A, Serbanescu[2]

[1]Gipsa-lab, Universite Grenoble Alpes, 11 rue des Mathematiques BP 46, 38402 Saint Martin D'Heres, France
[2]Military Technical Academy, Department of Communications and Military Electronic Systems,39-49 George buc Avenue, 050141 Bucharest, Romania
[3]National Institute for R&D in Electric Engineering ICPE-CA, 313 Splaiul Unirii, 030138 Bucharest, Romania
[4]Laboratoire de Machines Hydrauliques, Universite de Laval, Loc.1341 Pav. Adrien-Pouliot, Quebec, QC, Canada G1V 0A6
[5]Power Engineering Faculty, "Politehnica" University of Bucharest, Romania, 313 Splaiul Independentei, 060042 Bucharest, Romania

E-mail: angela.digulescu@mta.ro

Abstract. In hydraulic turbines operating at part loads, a cavitating vortex structure appears at runner outlet. This helical vortex, called vortex rope, can be cavitating in its core if the local pressure is lower that the vaporization pressure. An actual concern is the detection of the cavitation apparition and the characterization of its level. This paper presents a potentially innovative method for the detection of the cavitating vortex presence based on acoustic methods. The method is tested on a reduced scale facility using two acoustic transceivers positioned in "V" configuration. The received signals were continuously recorded and their frequency content was chosen to fit the flow and the cavitating vortex. Experimental results showed that due to the increasing flow rate, the signal - vortex interaction is observed as modifications on the received signal's high order statistics and bandwidth. Also, the signal processing results were correlated with the data measured with a pressure sensor mounted in the cavitating vortex section. Finally it is shown that this non-intrusive acoustic approach can indicate the apparition, development and the damping of the cavitating vortex. For real scale facilities, applying this method is a work in progress.

1. Introduction

Due to the present conditions in the energy market, the hydraulic turbines are frequently required to operate far from the optimum operation regime. Usually, at partial flow rate operation, a helical vortex appears in the turbine draft tube which can be cavitating in its core. The effects are undesirable pressure fluctuations and vibrations which can affect the operation of the turbine and the entire hydraulic circuit. This is why is important to detect such phenomena before the effects produce irreversible damage to the machine or hydraulic circuit.

The present paper continues the research on the detection of the cavitating vortex based on non-intrusive active devises like the acoustic transducers. In previous works, the influence of the vortex rope presence over the acoustic signal bandwidth was analyzed [1] and different acoustic

transducers configuration were used [2]. The results of both works mentioned above suggested that acoustic techniques could be robust and efficient methods for detection of cavitating vortex presence in flow through hydraulic machinery.

In the present work the objective is to emphasize the effect of the cavitating vortex upon the recorded signal in order to identify the different phases of evolution of the phenomenon using two pairs of acoustic transducers. Measurements were carried out on a laboratory facility which simulates the flow conditions downstream a hydraulic turbine. The Recurrence Plot Analysis (RPA) method was applied on the recorded signals in order to characterize the state of the flow in its evolution.

This paper is organized in five parts. After the introduction in section 1, section 2 presents the relation between the vortex flow and spectrum. Because the received Doppler spectrum is clearly related to the spatial velocity distribution of a Rankine vortex [3], the research will begin from this aspect. Further, section 3 describes the RPA method and highlights the quantification of the diagonal lines specific for the recurrence matrix. More, an interesting approach of the spectral analysis of the diagonal lines is presented. The experimental works and results are discussed in section 4, followed by the conclusions and perspectives in section 5.

2. The vortex flow and vortex spectrum

In literature the vortex vector is defined as $\nabla \times u = 2\omega$, where ω is the rotational speed of the fluid. The flow for an incompressible fluid of velocity u is described by the Navier-Stokes (1) and continuity equations (2) [3, 4]:

$$\frac{\partial u}{\partial t} + u \cdot \nabla u = -\frac{1}{\rho}\nabla p + v\nabla^2 u \tag{1}$$

$$\nabla \cdot u = 0 \tag{2}$$

where p is the fluid pressure, ρ is the density of the fluid, u is the flow velocity vector, v is the flow viscosity and ∇ is del operator.

For vortex analysis, the Rankine model can be used. Analytically, the Rankine vortex is defined by the components from (3) [5]:

$$u_r = 0; u_z = 0; u_\theta = \begin{cases} \frac{r}{r_{max}} v_{max}, r \leq r_{max} \\ \frac{r_{max}}{r} v_{max}, r > r_{max} \end{cases} \tag{3}$$

where u_r, u_z and u_θ are the axial, radial and, respectively, tangential velocity components defined in a cylindrical coordinate system for the u flow velocity. It should be mentioned that, when $r \leq r_{max}$, the tangential velocity u progresses in the forced vortex region, while, when $r > r_{max}$, its progress happens in the free vortex region.

The frequency signature of the cavitating vortex is given by the solution (3) of equations (1) and (2) through the solution ω. Hereby, the relation between the vortex flow and its spectrum is:

$$u_r = 0; u_z = 0; u_\theta = \begin{cases} \omega \cdot r, r \leq r_{max} \\ \frac{\omega \cdot r_{max}^2}{r}, r > r_{max} \end{cases} \tag{4}$$

In [5], there can be found more details about the spectral magnitude of Doppler velocity.

3. Recurrence Plot Analysis

The nonlinear time series analysis that characterizes the general dynamic system is used for the signal processing of nonlinear systems. This method has its origins in the nonlinear time series analysis which begins with a time series obtained from a measured set of data:

$$\mathbf{x} = \{x[1], x[2], ..., x[N]\} \tag{5}$$

which is represented in a m-dimensional space, named the phase space where m is the embedding dimension. The following vectorial representation gives the trajectory represented in the phase space:

$$\vec{v_i} = \sum_{k=1}^{m} x[i + (k-1)d] \cdot \vec{e_k}, i = \overline{1, M} \tag{6}$$

where $x[\cdot]$ is the sample from the time series (5), $\vec{e_k}$ are the unit vectors of the axis of the phase space, $M = N - (m-1)d$,d is the delay parameter. The values for parameters d and m are important and chosen, in a manner which will be detailed.

Using the RPA method, the distance/reccurrence matrix is determined after the trajectory is obtained [6]. A certain type of distance between two points i and j on the trajectory is used to obtain the matrix, each distance being compared with a threshold:

$$D_{i,j} = \Delta(v_i, v_j) \tag{7}$$

$$R_{i,j} = \Theta(\varepsilon - \Delta(v_i, v_j)) \tag{8}$$

where $D(i,j)$ is the element of the distance matrix corresponding to the points i and j, $\mathcal{D}(\cdot,\cdot)$ is the type of distance applied on the trajectory points (Euclidean distance, norm L1, norm infinity, angular distance, etc.), $R_{i,j}$ is the element of the recurrence matrix, ε is the threshold which determines whether or not two points i and j are recurrent and Θ is the Heaviside step function. Generally, ε is constant.

The representation of the distance matrix is done by a continuous colored scale, while for the representation of the recurrence matrix values 0 and 1 are used, colored in black and white [7].

The quality of the trajectory is directly influenced by the delay parameter, d [8]. A small value of the delay will make the trajectory redundant (the trajectory is overly folded around the first bisector of the phase space). A too large value of the delay, will make the trajectory irrelevant (being too complicated).

The embedding dimension m, must be considered in comparison to the real dimension of the representation. If it is smaller, this trajectory would be a projection of the real trajectory which would include points closer to each other than on the real trajectory. If the embedding dimension is greater than the real one, then the computation resources and time would increase significantly. So, in order to choose the optimal value, the False Nearest Neighbor (FNN) method will be used [6, 8, 9], and this value will be determined by the first value of FNN equal to zero.

It follows the quantification of the diagonal lines on the distance matrix, as presented by [10].

$$sd[n] = \frac{1}{M-n} \sum_{i=1}^{M-n} D(i,j) \tag{9}$$

where M is presented below equation (6), $n = \overline{0, M-1}$ and $D(v_i, v_{i+n})$ are the elements of the n^{th} diagonal line of the recurrence matrix (the 0 diagonal corresponds to the main diagonal).

Furthermore, the Fourier transform is applied on the diagonal lines quantification:

$$SD[k] = \sum_{n=0}^{M-1} sd[n] \cdot exp\left(\frac{-i2\pi kn}{M}\right) \tag{10}$$

This method has an important advantage, because it highlights several extra frequency components than the usual Fourier transform. In order to support this statement the mathematical operations will be presented in a general matter. Considering the following time series:

$$x[n] = \cos(\Omega n) \cdot \cos(\omega n), \Omega \gg \omega \tag{11}$$

the interaction between the acoustic wave characterized by the spectral parameter Ω and a rotational vortex characterized by ω is presented in a simple way.

The argumentation is done on a time series represented in two dimensions (so the embedding dimension, m is 2) and the evaluation is done with the distance matrix using the squared Euclidean distance:

$$\vec{v_i} = x[i] \cdot \vec{e_1} + x[i+d] \cdot \vec{e_2} \tag{12}$$

$$D(i, i+n) = (x[i] - x[i+n])^2 + (x[i+d] - x[i+d+n])^2 = E_i^2(n) + E_{i+d}^2(n) \tag{13}$$

Equation (11)is introduced in equation (13) and it results:

$$E_i(n) = 2\alpha \cdot \sin\frac{\Omega[2i+n]}{2} \cos\frac{\omega[2i+n]}{2} \tag{14}$$

where $\alpha = \frac{\sin(\Omega+\omega)}{2} \cong \frac{\sin(\Omega-\omega)}{2}$ considering that $\Omega \gg \omega$.

The results from equation (14)are replaced in equation (13):

$$\begin{aligned} sd[n] \propto D(i, i+n) \cdot \alpha^{-2} = 1 + \cos\left[2\omega\left(i + \frac{n}{2}\right)\right] - \cos\left[2\Omega\left(i + \frac{n}{2}\right)\right] \\ - \cos[\Omega(2i+n)] \cdot \cos[\omega(2i+n)] + 1 + \\ \cos\left[2\omega\left(i + d + \frac{n}{2}\right)\right] - \cos\left[2\Omega\left(i + d + \frac{n}{2}\right)\right] \\ - \cos[\Omega(2i+2d+n)] \cdot \cos[\omega(2i+2d+n)] \end{aligned} \tag{15}$$

Equation (15), shows that besides the classical components $\Omega \pm \omega$, two extra components appear on the spectral representation of the diagonal lines quantification, one component at 2Ω and the other at 2ω.

Further, the experimental part aims to emphasize the evolution of the cavitating vortex considering that the effect of the vortex can be attributed to the 2ω spectral component.

4. Experimental Setup and Results

The measurements were done on the experimental set-up from [1, 2], but in a different configuration. A stator is pused to create a cavitating vortex rope, similar with vortex ropes often met in hydropower plant turbines, as presented in figures 1 and 2 [11]. The stator is placed 70 mm upstream the divergent section (previously, it was situated at 250 mm). For the acoustic analyse, two pairs of transceivers positioned in 'V' configuration were used (figures 1 and 2) instead of only one. Moreover, the transducers were placed further downstream from the cavitating vortex area, on the divergent section (figure 1), while in the previous studies they were placed on top of the cavitating vortex area. The acoustic transceivers have a wide band reception centered on 1MHz, but being able to receive signals in the range $800 - 1200$kHz. The output signal varies from $-20V$ to $20V$. The transceivers were set in active configuration and the acquisition was made at a sampling frequency of $20MHz$ for bursts of $1ms$ with the repetition rate of $2.6ms$. Also, besides the acoustic and discharge flow, the pressure was measured on the bottom side of the pipe, in the cavitating vortex area (right downstream the stator) using an absolute pressure transducer of 0...1 bar.

The experimental set-up is designed to create the conditions for a cavitating vortex to appear and develop while increasing the discharge to the maximum flow capacity of the set-up. The

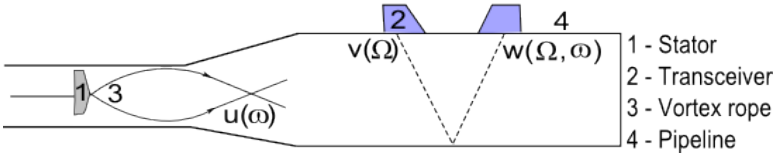

Figure 1: The longitudinal representation of the measuring section

(a) (b)

Figure 2: The experimental setup

first set of data was obtained for the appearance and developing of the cavitating vortex during discharge increase. In order to cover the damping behavior of the cavitating vortex from a hydraulic turbine, the variation of the discharge was reversed in the set-up, so the effect of the cavitating vortex disappearance was created.

The acoustic transceivers operate around at $1MHz$ and the emitted waveform is a wide band signal with the same central frequency. This signal, $u(\Omega)$ has a cubic characteristic law. As figure 2 shows, two of the transceivers were used as emitters and the other two as receivers. One emitted in the flow direction and is characterized by a cubic law, whereas the other emitted in the opposite direction and had an inverse cubic law.

The experiment was done while slowly varying the flow rate of the water. In other words, during the experiment the received signal is acquired and recorded in bursts of 2.6 ms simultaneously with the flow rate and the pressure of the water.

Considering that the cavitating vortex is characterized by an unknown law $v(\omega)$ and the wide band signals (that are continuously emitted) are characterized by the $u(\Omega)$, then, at the receiver, the signal carries the interaction between the emitted signal and the studied cavitating vortex in $w(\Omega, \omega)$. The purpose of the experiment is to highlight the signature of the cavitating vortex from the received signal and to compare the results with the ones obtained in different configuration.

The wide band acoustic signals transmitted during the experiment were chosen to characterize as good as possible the flow and the cavitating vortex in order to highlight the apparition, development and damping of the vortex. During the experiment, the water flow was varied from 6 to $19l/s$ and backwards, in order to determine the critical flow rates for which the cavitating vortex appears/dampens.

The first set of data was obtained for water flow rate increase, when the apparition and developing of the cavitating vortex occurred. Based on the visual observation (figure 3), three stages of the vortex evolution were identified : A_1 region no vortex presence (up to $6l/s$), A_2 region incipient vortex (from 6 to $7.2l/s$) and A_3 region developed vortex (more than $7.2l/s$).

Using the property of the RPA spectral analysis, the position of the 2ω component from the

(a) A1 (b) A2 (c) A3

Figure 3: Cavitating vortex stages: A_1 no vortex, A_2 incipient vortex, A_3 developed vortex

absolute value of SD (the amplitude spectrum of sd - eq. (9)) was determined for each burst of $2.6ms$ in each vortex region. Further, an example of 2ω component identification is presented in figures 4 and 5. In figures 4 and 5 the main component at $1MHz$ corresponds to the central frequency of the emitted signal at the acoustic sensors. Other significant components can be found in the range of $0-100kHz$ (based on the demonstration from eq. (15)), and are attributed to 2ω component, as presented in the zoomed details (figures 4b and 5b).

The frequencies corresponding to the 2ω component (eg. in figures 4b and 5b for region A_1 at $20.14kHz$, respectively for A_3 at $49.44kHz$) are further presented as the time variation of the 2ω spectral component in figures 6a and 6b. Also, the flow variation was represented simultaneous with time variation of 2ω spectral component in order to identify the three cavitating vortex regions.

The normalization of the parameters presented in the following figures is done using the maximum value of each data vector.

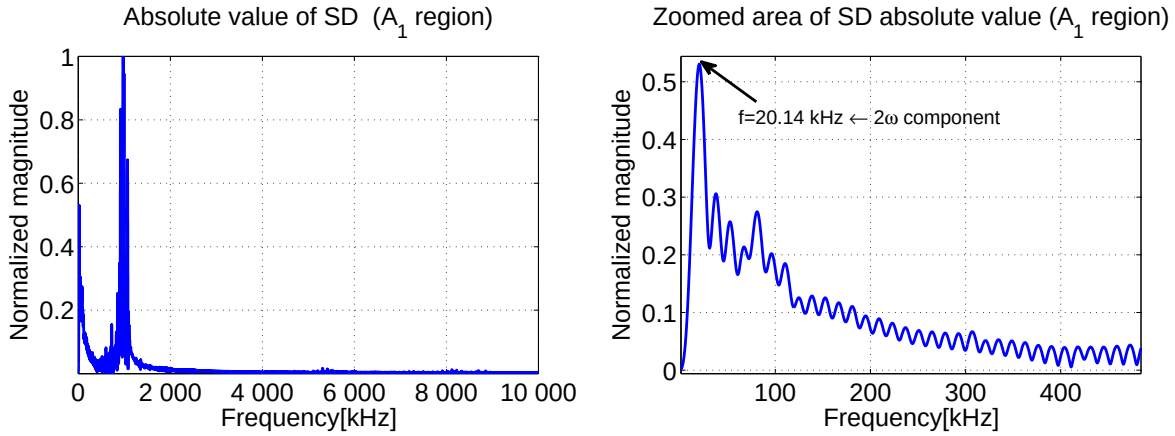

(a) The amplitude spectrum of A_1 region (b) Zoomed amplitude spectrum of A_1 region

Figure 4: SD absolute value for an acquisition of $2.6ms$ in A_1 region

For the increasing flow rate configuration, it can be seen that, while there is no vortex (A_1 region), the 2ω component has a reduced variation. When the vortex starts to appear in A_2 region, the deviation of the 2ω is larger and is significantly increasing in A_3 region for the developed vortex. The standard deviations of the 2ω component, $\sigma_{2\omega}$, for each region were computed, and cavitating vortex characterization criteria were defined according to them (table 1).

The validation of the criteria was firstly done using data recordings during decreasing water flow configuration. The 2ω component was determined and its time variation was plotted

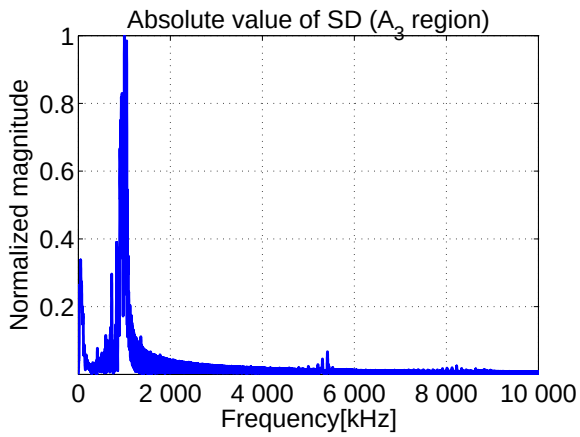

(a) The amplitude spectrum of A_3 region

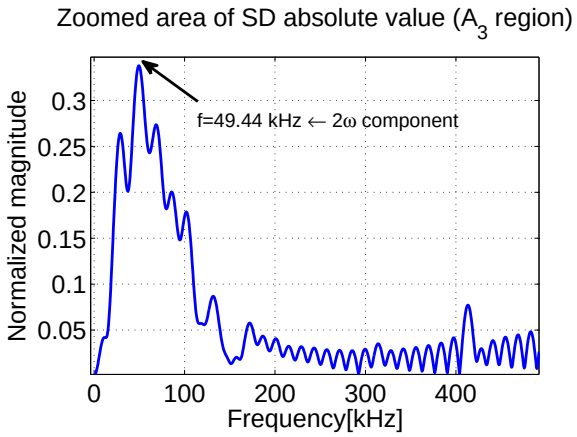

(b) Zoomed amplitude spectrum of A_3 region

Figure 5: SD absolute value for an acquisition of $2.6ms$ in A_3 region

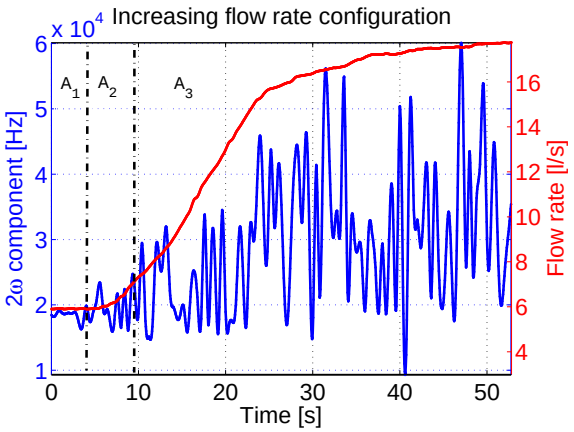

(a) Time variation of 2ω component and flow rate during increasing regime

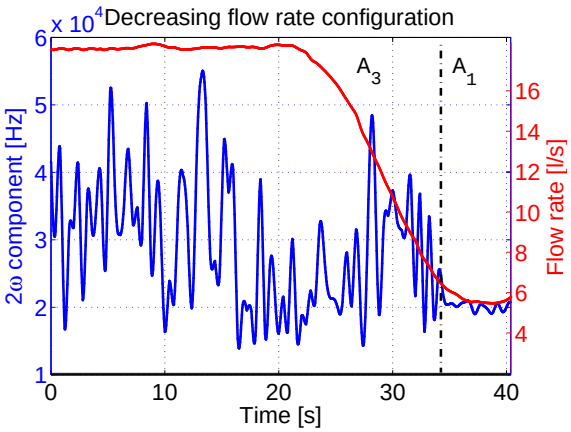

(b) Time variation of 2ω component and flow rate during decreasing regime

Figure 6: Time variation of 2ω component (in blue) and the flow rate evolution (in red)

Table 1: Criteria limits for the cavitating vortex stages classification in increasing flow rate configuration

Region	$\sigma_{2\omega}$[kHz]	Limits[kHz]	Vortex stage
A_1	0.76	$\sigma_{2\omega} < 1$	No vortex
A_2	2.26	$1 \leq \sigma_{2\omega} \leq 3$	Incipient vortex
A_3	9.71	$\sigma_{2\omega} > 3$	Developed vortex

together with the water flow variation in figure 6b. The cavitating vortex regions were identified by visual observations and fitted with the defined criteria (table 2). In this case, the incipient vortex stage (A_2 region) was not visible, which was also confirmed by the high value of standard deviation of the 2ω component computed. This may be caused by the inertia of the fluid while decreasing the flow, which was done in a shorter period than in the increasing case (about $15s$

Table 2: Criteria validation for decreasing flow rate configuration

Region	$\sigma_{2\omega}$[kHz]	Vortex stage
A_1	0.74	No vortex
A_2	–	–
A_3	9.13	Developed vortex

Table 3: Validation of vortex regions with experimental data obtained in different configuration [2]

Region	$\sigma_{2\omega}$- increasing flow[kHz]	$\sigma_{2\omega}$- decreasing flow[kHz]	Vortex stage
A_1	0.81	0.73	No vortex
A_2	2.15	2.29	Incipient vortex
A_3	5.98	7.08	Developed vortex

comparing to $30s$).

Furthermore, experimental results obtained in our previous work for a different configuration of the cavitating vortex generator and acoustic sensors [2], were used for criteria validation. The vortex stages identified in [2] for increasing and decreasing flow variations fitted the limits defined in table 1, so confirming the criteria as presented in table 3.

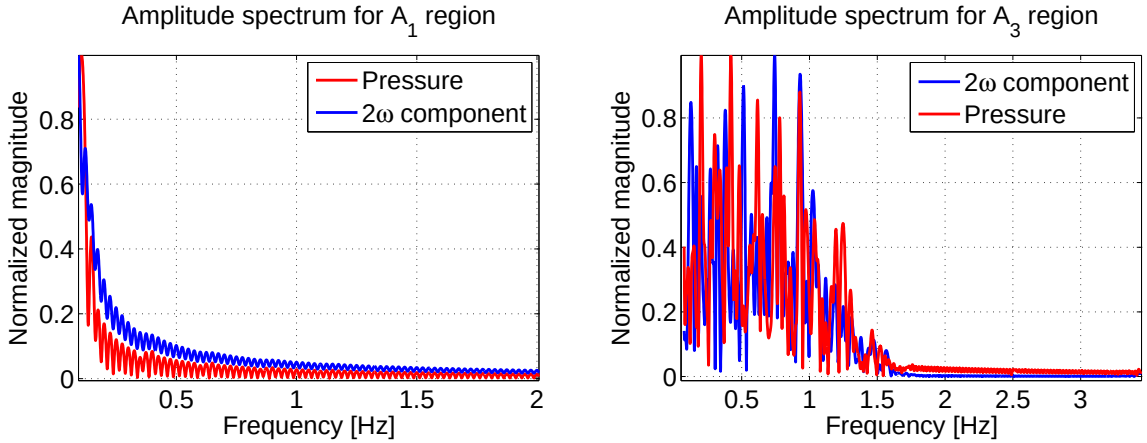

(a) The normalized amplitude spectrum for the A_1 region

(b) The normalized amplitude spectrum for the A_3 region

Figure 7: The normalized amplitude spectrum in the increasing flow configuration

The spectral analysis of 2ω and pressure variation showed the same spectral distribution of the components for the two main regions $A1$ (figure 7) and A3 (figure 8). Figures 7a and 8a clearly show that in the developed vortex regime the distribution of the spectral components is amplified for the low frequencies for both acoustic and pressure variations, which is characteristic for vortex flows. Therefore the new signal processing tool is able to characterize the vortex in its evolution.

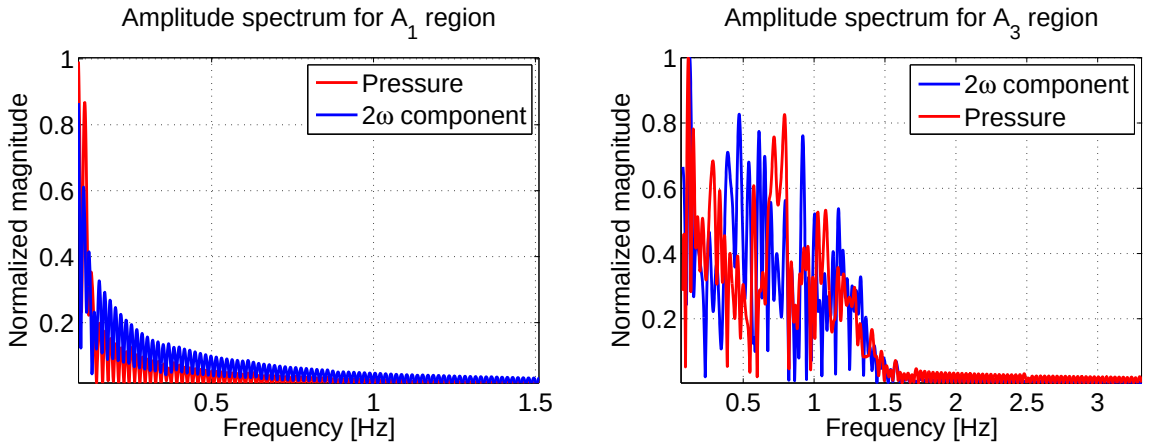

(a) The normalized amplitude spectrum for the A_1 region

(b) The normalized amplitude spectrum for the A_3 region

Figure 8: The normalized amplitude spectrum in the decreasing flow configuration

5. Conclusions

This paper presents a new tool capable to characterize the presence of cavitating vortex flow (as in hydraulic turbines), using a non-invasive acoustic technique, easy to set up in experimental and industrial sites.

The experiment was done by varying the flow rate from $6\frac{l}{s}$, without cavitating vortex to a flow rate of $19\frac{l}{s}$, where the vortex is clear eye visible, as presented in figure 2.

This paper presents the RPA method, specific for chaotic systems, and, in order to detect the cavitating vortex signature, we have proposed the analysis of the spectral components of the diagonal lines quantification.

The diagonal lines reflect the fundamental frequency of a signal [6]. Moving forward, in this paper, it is described the spectral analysis of these diagonal lines quantification which brings into light the effect of an interaction between two different waves, in certain conditions.

The theory was confirmed by the experimental tests: the cavitating vortex signature is present in the spectral components of the diagonal lines quantification. This component describes the evolution of flow and of the cavitating vortex.

For the future research, a single pair of acoustic sensors will be used, as the use of two pairs induced interference in the received signals. Also, they will be set above the cavitating vortex area in order to try quantifying the vapor volume within the flow.

Acknowledgments

The French part has been funded by the FUI Tenerrdis - Minalogic project "Smart Hydro Monitoring". The Romanian part has been funded by the Executive Agency for Higher Education, Research, Development and Innovation, PN-II-PT-PCCA-2013-4, no. 88/2014, ECOTURB project.

References

[1] Candel I, Bunea F, Dunca G, Bucur D M, Ioana C, Reeb B, Ciocan G D, 2014,Detection of cavitation vortex in hydraulic turbines using acoustic techniques, *J. Phys.: Conf. Series - Earth and Environmental Science, 22*, 052007

[2] Digulescu A, Petrut T, Candel I, Bunea F, Dunca G, Bucur D M, Ioana C, Serbanescu A, 2014, On the vortex parameter estimation using wide band signals in active acoustic system, *OCEANS '14 MTS/IEEE Taipei - Ocean Regeneration*, pp. 1-5

[3] Takahashi N, Miyazaki T, 2006, The Influence Of Turbulence On A Columnar Vortex With Axial Flow, *Proc. in Applied Mathematics and Mechanics, PAMM*, pp. 879-882
[4] Emanuel K A, 1984, A Note on the Stability of Columnar Vortices, *J. of Fluid Mechanics, 145*, pp. 235-238
[5] Rubin W L, 2000, Radar-Acoustic Detection of Aircraft Wake Vortices, *Journal of Atmospheric and Oceanic Technology, 17*, pp. 1058-1065
[6] Marwan N, Schinkel S, Kurts J, 2013, Recurrence plots 25 years later Gaining confidence in dynamic transitions, *Europhysics Letters, 101*, 20007
[7] Ioana C, Digulescu A, Serbanescu A, Candel I, Birleanu F M, 2014, Recent Advances in Nonstationary Signal Processing Based on the Concept of Recurrence Plot Analysis, *Springer Proc. in Mathematics & Statistics, M. Marwan et al. (Eds.): "Translational Recurrences"*, pp. 75-93
[8] Thiel M, Romano M C, Kurths J, Meucci R, Allaria E, Arecchi T, 2002, Influence of the observational noise on the recurrence quantification analysis, *Phisica D; 171* pp. 138-152
[9] Small M, 2005, Applied nonlinear time series analysis. Applications in phisics, physiology and finance, *World Scientific Publishing*
[10] Birleanu F M, Candel I, Ioana C, Gervaise C, Serbanescu A, Serban G, 2012, A vector approach to transient signal processing, *11th Int. Conf. on Information Science, Signal Processing and their Applications*, pp.1174-1179
[11] Bunea F, Ciocan G D, 2015, Test bench for study of rotational biphasic flow study with adverse pressure gradient, *Patent application registration, OSIM no. A/00704/29.09.2015*